Engineered Science
DOI: https://dx.doi.org/10.30919/es8d1142

Chemical Bath Deposition of $CuInS_2$ Thin Films and Synthesis of $CuInS_2$ Nanocrystals: A Review

J. P. Sawant,[1] Shoyebmohamad F. Shaikh,[2] R.B. Kale[3] and H. M. Pathan[4,*]

Abstract

Thin-film and nanocrystal copper indium disulfide (such as $CuInS_2$, CIS) gained significant attention in academics and industry due to their fascinating optoelectronic properties. Numerous studies have reported the deposition of CIS thin-films and the synthesis of nanocrystals using various techniques. Chemical bath deposition (CBD) method and the environmental friendly hydrothermal method offer the best option for the deposition of $CuInS_2$ thin films and synthesis of $CuInS_2$ nanocrystals respectively, in a cost-effective way. The fabrication of CIS-based thin-film solar cells using low-cost and simple way can be one of the promising alternatives to silicon solar cells. This review article described the physical and chemical properties of CIS thin-films deposited by the CBD method and hydrothermal synthesized CIS nanocrystals.

Keywords: CIS thin films: Chemical bath deposition; Hydrothermal method; Light absorber layer, Solar cell.
Received: 16 August 2020; Accepted: 25 October 2020.
Article type: Review article.

1. Introduction

World energy demand is increasing day by day. Today, non-renewable energy sources such as petroleum, coal, hydrocarbon gas, natural gas, nuclear energy, etc are the most commonly used energy sources. These energy sources are limited, extracted from the earth, and will eventually run out with time. In the current scenario, worldwide crude oil production is more than 100 million barrels per day (Mb/d) by the mid-2020. It will reach 104 and 118 Mb/d in 2030 and 2050, respectively.[1] If we continuously use fossil fuel at the current rate, the earth will be running out of natural gas within 65 years, coal in about 200 years, and petroleum within 50 years.[2,3] Also, the emission of carbon dioxide and the final product of fossil fuel significantly influence the earth's atmosphere. Therefore, it is important to find other alternatives to these energy resources. Because of the limited availability of nonrenewable energy resources and the impact on global warming, alternative renewable energy options are required. Renewable energy sources can be the alternative to nonrenewable sources. The renewable energy sources used for energy production are mainly solar energy, wind energy, geothermal energy, hydropower energy, and ocean energy in the form of water waves (Fig. 1). Throughout the decades, there has been a great deal of work to establish new renewable energy sources. One of the most promising alternatives is to harvest solar energy, an abundantly available, clean, and green energy source through solar cells.[4-8] The solar energy can be harvested through solar cells. In this regard, a variety of chalcopyrite materials such as copper indium disulfide/selenide ($CuInS_2/Se_2$ – CIS/Se), and copper indium gallium sulfide/selenide ($Cu(In,Ga)S_2/Se_2$ (CIGS/Se), $CuFeSe_2$ have been used in solar cells as a light-absorbing layer and technology is being developed to enhance efficiency by reducing costs and toxicity, etc.[9,10]

Among various absorber materials used in the solar cell, the ternary copper indium disulfide ($CuInS_2$, CIS) compound semiconductors have attracted much attention. Because of the interesting optoelectronic properties, CIS can be used in applications like solar cells, photoelectrochemical cells (PEC), photodetectors and light-sensing transistors, etc. [10,11] The CIS is a ternary semiconductor (I–III–IV_2) that contains nontoxic materials, with a direct bulk bandgap between 1.3 and 1.5 eV,[8,12-14] and a high optical absorption coefficient of about 10^5 cm^{-1}. The CIS can be obtained in both n-type and p-type since its conduction type depends on the intrinsic defects, such as cation vacancies and anti-site defects.[15] Theoretically, photoconversion efficiency around 27-32% has been

[1] *Department of Physics, University of Mumbai, Santacruz (E), Mumbai – 400098, India*
[2] *Department of Chemistry, College of Science, King Saud University, Riyadh 11451, Saudi Arabia*
[3] *Department of Physics, Institute of Science, Madam Cama Road, Fort, Mumbai 400032, India*
[4] *Advanced Physics Laboratory, Department of Physics, Savitribai Phule Pune University, Pune- 411 007*
* *Email:* pathan@physics.unipune.ac.in (Dr.H. M. Pathan)

calculated for CIS absorber layer[16, 17] and it is nearly equal to other chalcopyrite materials used in solar cells. Polycrystalline CIS laboratory solar cell has been produced with an efficiency at almost 13 percent.[18] The CIS thin films can be deposited by chemical methods such as chemical bath deposition (CBD),[19-21] spray pyrolysis,[22,23] electrodeposition,[24,25] successive ionic layer adsorption and reaction (SILAR)[26,27] as well as physical method like co-evaporation from elemental source,[28,29] molecular beam epitaxy,[30,31] sputtering,[32,33] chemical vapor deposition (CVD),[34,35] laser chemical vapor deposition (LCVD),[36] atomic layer deposition,[37] etc.

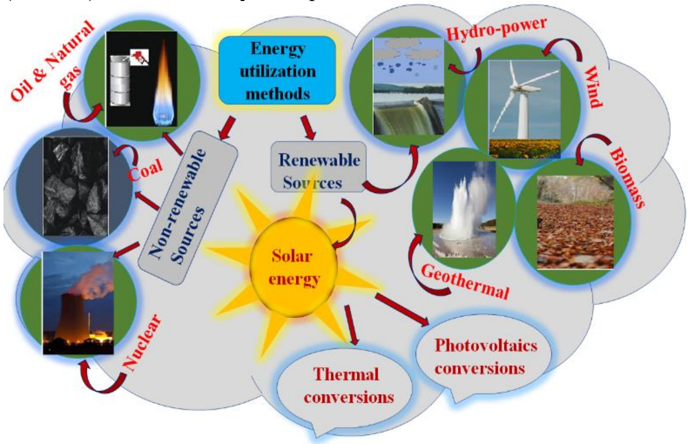

Fig. 1. Different energy utilization methods.

Although the deposition of thin films via the aforementioned physical methods results in good-quality thin films, it is highly expensive and requires many material targets. Therefore, an alternative low-cost method is needed to produce good quality films. Chemical deposition methods could be the best alternative because most of them do not require expensive equipment. The chemical method strongly depends on the deposition parameters such as solution chemistry, solution concentration, pH value, solution temperature, etc.

Among all the chemical methods, the CBD method has attracted considerable interests because of its simplicity. It does not require a sophisticated instrument. Low operating temperatures, large-area deposition, and flexibility in the selection of substrate are other advantages of the CBD method. In this review article, we briefly discussed CBD methods for the deposition of a ternary CIS thin film. Their preparative parameters, structural, morphological, and electrical properties were described. The properties CIS nanocrystals synthesized using simple and low-cost hydrothermal method also discussed. The data on preparative parameters of the CIS thin films and hydrothermal synthesized CIS nanocrystals from the previously published reports have been presented in tabular form.

2. Crystal structure of $CuInS_2$

The $CuInS_2$ is a chalcogenide ternary semiconductor material, which belongs to the I-III-VI_2 group. Its molecular formula is ABX_2 and exhibits a tetragonal crystal structure (A= Cu, Ag, B= Al, In Ga and X=S, Se, Te). It is an isoelectronic analog of binary (II-VI) semiconductors. The crystal structure of ternary chalcopyrite belongs to the nonsymmorphic space group D_{2d}^{12} with eight atoms per primitive unit cell.[38] It is the superlattice structure of zinc blend or sphalerite structure, which has a diamond like unit cell consisting of two inter-penetrating face centered cubic lattices, separated by translational vectors of (1/4, 1/4, 1/4) consisting of two atoms per primitive unit cell.[38] The chalcopyrite cell structure of the CIS consists of eight atoms per unit cell. Each cation (A, B) is tetrahedrally coordinated by four anions (X), whereas each anion (X) is coordinated tetrahedrally by two cations (A, B) in an orderly manner.[39]

The difference between zinc blend structure and chalcopyrite structure is the existence of two cation sub-lattices, i.e., tetrahedral distortion and anion displacement. The presence of two different cations in ternary chalcopyrite results in two near-neighbor chemical bands (A-X, B-X) with unequal bond lengths ($R_{A\text{-}X} \neq R_{B\text{-}X}$). The tetragonal distortion existing in the structure is mainly due to two different cations forming two chemical bonds of different bond lengths. Because of this, the tetragonal cell gets distorted leading to the distortion ($\eta = c/2a \neq 1$), where a and c correspond to the lattice parameters of the diagonal unit cell.[38] Due to the anion displacement (u) from the ideal tetrahedra site, the bond length mismatch is observed, which does not exist in the zinc blend-like undistorted anion sublattice. Because of theses added structural (η, u) and chemical degrees of freedom, the ternary chalcopyrite structure exhibits superior physical and chemical properties relative to their binary analog.

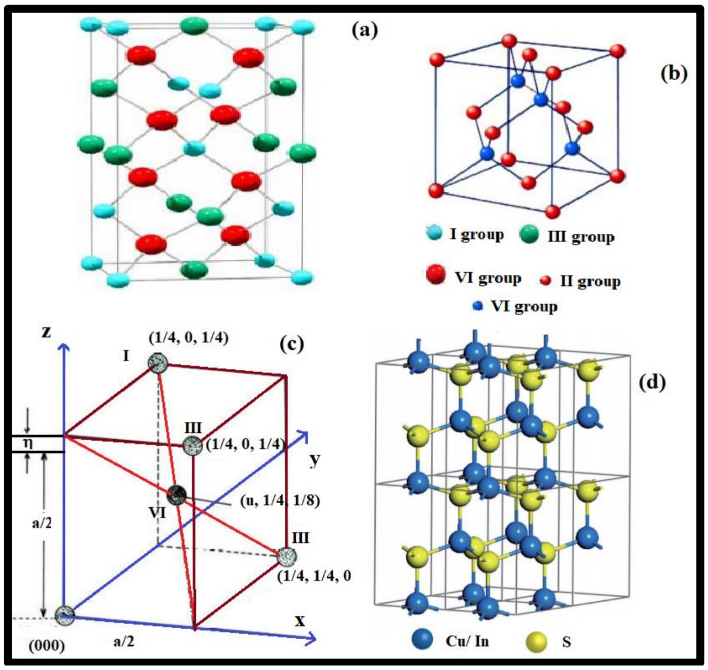

Fig. 2 a) Tetragonal unit cell of chalcopyrite $CuInS_2$, b) zinc blend or sphalerite unit cell, c) tetragonal distortion (η) and anion displacement (u) in $CuInS_2$ unit cell, and d) wurtzite unit cell.

Table 1. Physical Properties of the $CuInS_2$ (Bulk).[38- 43]

Sr. No.	Specification	Value
	Structural Properties	
1	Lattice parameters	a = b = 0.55 nm c = 1.01, c/a = 2.01
2	Crystal structure	Tetragonal (chalcopyrite, sphalerite and wurtzite)
3	Density	4.75 g/cc
4	Volume compressibility,	0.141 x 10^{-10} m²/N
	Electrical Properties	
1	Band gap energy	1.5 eV
2	Excitonic energy gap	1.554 eV
3	Carrier concentration (n-CIS) at RT	3×10^{16} cm^{-3}
4	Carrier concentration (p-CIS) at RT	6×10^{17} to 2×10^{18} cm^{-3}
5	Mobility (n-CIS) at RT	15 $cm^2V^{-1}S^{-1}$
6	Mobility (p-CIS) at RT	412 $cm^2V^{-1}s^{-1}$
7	Effective mass(m_p)	$1.3m_o$
8	Effective mass(m_n)	$0.03m_o$
	Optical Properties	
1	Refractive index	3.32
2	Extinction coefficient	0.0201
3	Optical energy gap (E_g)	1.5 eV
4	Real ε_1 dielectric constants	11.03
5	Imaginary ε_2 dielectric constants	0.134

The unit cell of chalcopyrite structure, zinc blend structure, the distortion in tetragonal unit cell and the wurtzite unit cell structure is depicted in Fig. 2(a-d), respectively. The lattice parameters and the physical properties of bulk CIS are summarized in Table 1.

3. The CBD of $CuInS_2$ thin films and their properties

The CBD is the simplest method available for the deposition of a variety of semiconductor thin film. All that is needed for deposition purposes is a vessel, which contains the aqueous solution of the precursors. Using CBD method, a large number of binary and ternary compounds such as cadmium sulfide/selenide (CdS/Se), coper sulfide/selenide (CuS/Se), lead sulfide/ selenide (PbS/Se) zinc sulfide/selenide (ZnS/Se) copper indium sulfide/selenide ($CuInS_2/Se_2$), coper zinc tin sulfide/selenide (CZTS/Se), etc. have been deposited.[44]

In the CBD method, two steps involved in the formation of a solid phase from a precursor solution are the formation of nucleation and particle growth.[45] For precipitation to take place and to produce the stable phase (nucleation), some minimum number of ions or molecules are required in the solution. The necessary step for the precipitate is the formation of nucleation. The concept of nucleation in solution is that the molecular cluster formed undergoes rapid decomposition and the particles combines to form a film on the substrate. The formation of films also depends on deposition condition such as the bath temperature, stirring rate, pH, concentration of the solution, etc. The film growth may occur through ion condensation of material or through the adsorption of colloidal material from the solution on the substrate. The schematics of the CBD method is shown in Fig. 3.

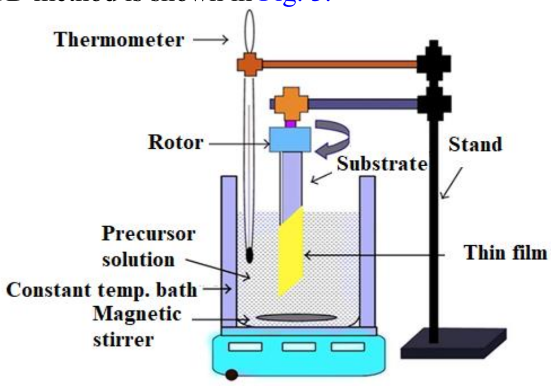

Fig. 3 Experimental set-up for chemical bath deposition.

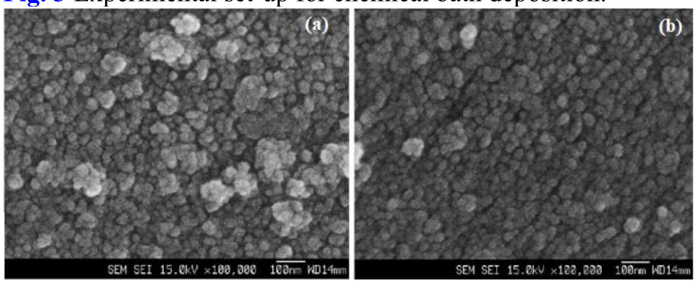

Fig. 4. The SEM image of CBD deposited CIS thin film a) as-deposited, b) annealed at 200 °C, reproduced with the permission from [47].

CIS is a strong candidate for thin-film photovoltaic cells. Because of the broad absorption coefficients, a CIS film of 1 µm thick is more than sufficient to absorb most of light in the visible spectrum. Several methods for depositing thin films of CIS have been reported. However, very few attempts have been made to deposit CIS by using the CBD method. For example, Padam *et al.*[19] reported the deposition of CIS thin films using cupric chloride ($CuCl_2.H_2O$) (0.5 M), indium chloride ($InCl_3$) (0.5 M) as an anionic precursor, and thiourea as a cationic precursor. Triethanolamine (TEA) was used as a complexing agent in the reaction. The effect of deposition temperature and deposition time on the physical properties of CIS thin films were investigated. The films deposited at 40 °C was reported to be a single-phase and well adherent to the substrate. Pathan *et al.*[46] employed a modified CBD (M-CBD) method to deposit stoichiometric CIS thin film. In a typical process, CIS thin films were obtained from the sequential deposition on the glass substrate in the mixture of anionic precursor and cationic precursor. The anions were complexed with TEA and hydrazine hydrate (HH)[47] Roh *et al.*[47] deposited CIS thin films on indium tin oxide (ITO) substrate. The SEM image of as synthesized and annealed CIS thin film showed compact and dense surface with a slight variation in the grain size (38 nm), which is depicted in Fig. 4. In the process, the adsorption of anions (Cu and In) and their reaction with cation (sulfur) and the compound film are formed on the substrate as shown in the following reaction.

$$Cu^{+} + In^{+3} + 2S^{-2} \rightarrow CuInS_2 \quad (1)$$

Gallium (Ga) doped CIS thin films were deposited on the ITO substrate by Pan *et al*.[48] To dope Ga, appropriate quantity of gallium trichloride ($GaCl_3$) was mixed in the TEA complexed precursor solution containing $CuCl_2.H_20$ (0.4 M), $InCl_3$ (0.5 M), and thioacetamide. A substitution of 0.2 M of Ga resulted in the transition of n-Ga-CIS to p-Ga-CIS. The carrier density increased with an increase in Ga concentration in the bath solution.

The slope of straight line in Mott-Schottky plot turned from positive to negative value, indicating the change of semiconductor property from n-type to p-type. The Ga doped compound semiconductor film showed a significant quantum efficiency, demonstrating that the films could be used for high-performance solar cells. In a further study, Garskaite *et al*.[49] have successfully deposited Zn, antimony (Sb) and Ni doped CIS thin films on the ITO substrate using CBD technique at room temperature. The XRD pattern depicted in Fig. 5 reveled that the crystalline nature of CIS thin film was improved with doping. The Mott-Schottky plot and the photocurrent density showed that the films make the transition from n-type to p-type conductivity for 0.6, 0.4, and 0.4 molar ratios of Zn, Sb, and Ni respectively. The doped films were employed in the reactor to study the hydrogen evolution. The maximum hydrogen evolution obtained was reported to be 33.26 mL/cm^2 with p-type Zn-CIS films. The surface morphological study of undoped and doped CIS thin films (Fig. 6) showed the uniform and dense surface with spherical grains over the surface.

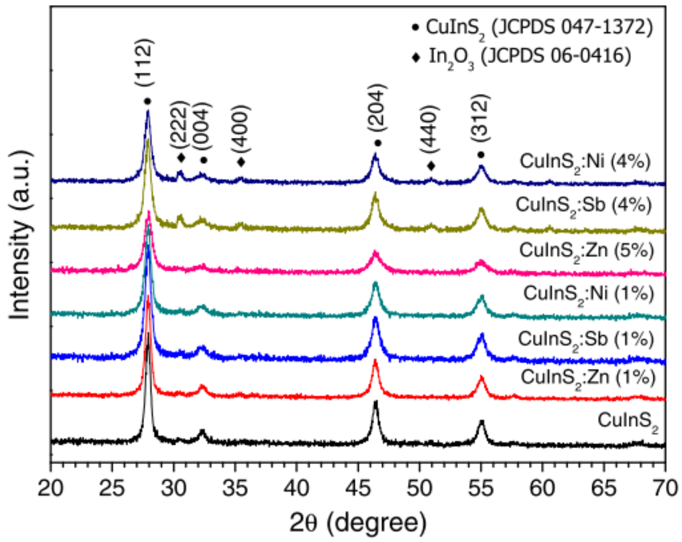

Fig. 5. The XRD patterns of undoped $CuInS_2$ and $CuInS_2$:Zn (1%), $CuInS_2$:Sb (1%), $CuInS_2$:Ni (1%), $CuInS_2$:Zn (5%), $CuInS_2$:Sb (4%) and $CuInS_2$:Ni (4%) films, reproduced with the permission from [49].

Comparative study of bandgap variation of thermally and chemically deposited CIS thin film was studied by Mahmoud *et al*..[50] Chemically as-deposited films were uniform, adherent. When the films were heated in a vacuum at 523 K, the grain size found to be increased. The study showed that the bandgap of the chemically as-deposited film was 1.5 eV. After annealing about 15 minutes at 623 K and 700 K in the sulfur atmosphere, the thermally deposited films showed a band gap of 1.52 eV. In sulfur atmosphere, reduction of the d-level contribution in the upper valence band and the change of lattice distance caused by nature of the native defects are mainly responsible for increase in the transition.[51]

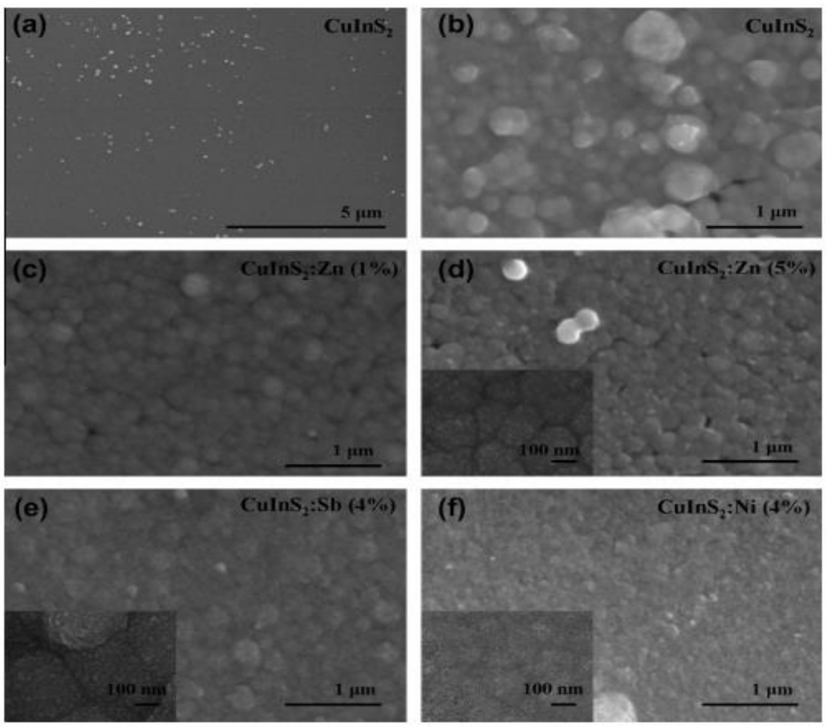

Fig. 6 The SEM images CIS thin film (a) and (b) without doping, (c) $CuInS_2$:Zn (1%), (d) $CuInS_2$:Zn (5%), (e) $CuInS_2$:Sb (4%) and (f) $CuInS_2$:Ni (4%). Insets in (d), (e) and (f) images show grain size of deposited films, reproduced with the permission from [49].

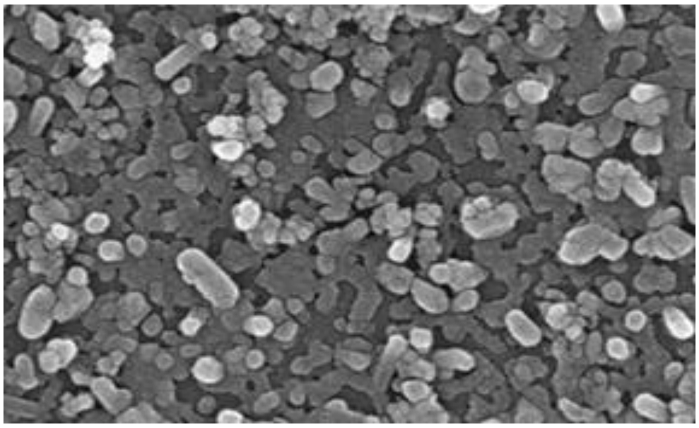

Fig. 7. SEM image of CIS thin film composed of nanorods on ITO substrate surface, reproduced with the permission from [53].

Bini *et al*.[52] have reported a novel method for the conversion of chemically deposited Cu_2S films into CIS film. The synthesis consists of evaporation of high purity indium on chemically deposited Cu_2S film. The XRD study of annealed Cu_2S sample (200 and 300 °C) showed an amorphous film. After evaporation of In on Cu_2S film, the obtained CIS film was converted into polycrystalline. The CIS nanorod thin films were synthesized in an alkaline medium.[53] Copper sulfate (0.02 M, $CuSO_4$), ammonia solution, indium chloride (0.02 M $InCl_3$), citric acid solution (0.05 M) and thiourea $(NH_2)_2$ CS (0.02 M) were used as the precursors for deposition, and TEA were used as a complexing agent. The ITO glass substrates were used for deposition and the deposition temperature was at 45 °C. The XRD study showed the tetragonal chalcopyrite phase with an intense peak at 37.32° orientation along the (211) crystal plane. Fig. 7 depicts the SEM image of CIS thin film, which shows the rod like CIS deposit on the substrate surface. The EDAX analysis revealed that the indium-rich stoichiometric composition (Cu-19.25%, In-65.87%, and S-14.88%) of CIS films. The optical study revealed that the band gap value of as-formed and aqueous ammonia etched CIS films was 1.40 and 1.46 eV respectively.

CIS thin films were formed by the sequential deposition of CBD-In_2S_3 and CBD-CuS thin films on glass using CBD method.[54] After heat treatment at 350 °C, In_2S_3-CuS thin-films completely were transferred to CIS film. The CIS thin film so formed was employed in the photovoltaic cell. The superstrate solar cell structure glass/SnO_2:F/CdS/Sb_2S_3/$CuInS_2$/PbS/C/Ag with CBD deposited CIS absorber layer showed a photo conversion efficiency of 0.53%. The photoconversion efficiency reported is low compared to the earlier reported values (2.35%),[55] where the CIS layer was deposited using chemical spray deposition method. The low photoconversion conversion efficiency could be due to the intermixing of the layers during the heat treatment. Cui *et al*.[56] recorded a Raman spectra of CBD deposited CIS thin film at approximately 290 cm^{-1} position, which belongs to chalcopyrite phase $CuInS_2$ (Fig. 8).

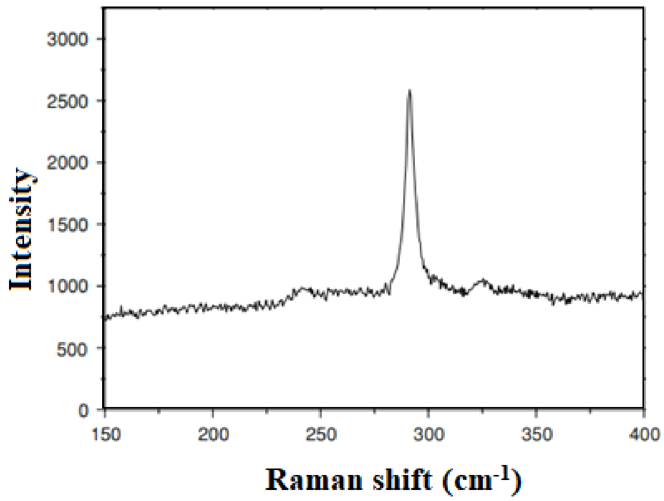

Fig. 8. Raman spectrum of annealed CIS thin film deposited using CBD method.

The formation of CIS thin films is probably related to the dissociation of the anionic complex and cationic complex.[45] In the CBD method, the complexing agent plays a vital role in the formation of thin films. During the deposition process, both the cations and anions present in the solution will react with each other and get converted into a neutral molecule. Due to this fast reaction, molecule precipitates before they deposit on the substrate. Therefore, to slow down the reaction rate, the anions were complexed with the complexing agent. In most of the reports, TEA was used as a complexing agent to form metal complexes. The thiourea, thioacetamide, and Na_2S were used as the sulfur (cationic) precursor.

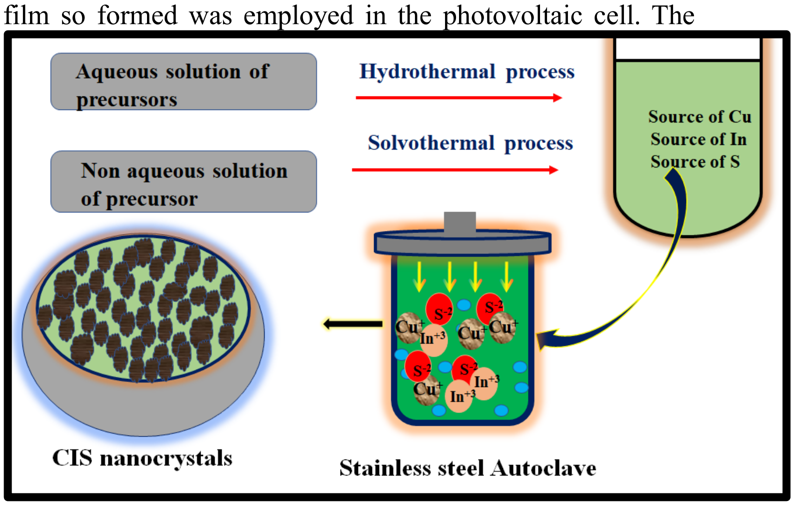

Fig. 9. The schematics of experimental set up of hydrothermal/solvothermal method for the preparation of CIS nanoparticles.

In an aqueous medium, the thioacetamide (CH_3CSNH_2-TAA) is ready to be dissociative in the following reaction,

$$CH_3CSNH_2 + H^+ \rightarrow H_2S + CH_3CNH^+ \quad (2)$$
$$H_2S + H_2O \rightarrow HS^- + H_3O^+ \quad (3)$$
$$HS^- + H_2O \rightarrow S^{-2} + H_3O^+ \quad (4)$$

The decomposition of TAA leads to the release of S^{-2} ions.

The step wise reactions involving the formation of metal complex in the presence of triethanolamine (TEA) are described as follows,

$$Cu^{+2} + TEA \rightarrow Cu(TEA)^{2+} \quad (5)$$
$$In^{+3} + TEA \rightarrow In(TEA)^{3+} \quad (6)$$

The Cu and In complexed ions and the sulfur ions migrate towards the surface of the substrate and the reaction take place to form $CuInS_2$ thin films as shown by the following reaction,

$$Cu(TEA)^{2+} + In(TEA)^{3+} + 2S^{2-} \rightarrow CuInS_2 \text{ film} \quad (7)$$

Uniform, adherent, desired stoichiometric and n or p conductive CIS film deposition is possible with the CBD technique. In many reports, the deposition of CIS is carried out at different deposition temperatures of solution precursors. The XRD patterns of room temperature deposited CIS film showed weak crystallinity/amorphous nature. Therefore, heat treatment was required for improving the grain size. Therefore, it is challenging to deposit thin films at room temperature with the desired stoichiometry. As a light absorber layer in the solar cell application, the required grain size of the CIS film must be around 1-2 µm. However, it is found difficult to obtain the required grain size of CIS material using CBD technique. To overcome these problems, deposition parameters should be properly optimized so that the CBD grown CIS films should be competent with that of other high cost and more effective depositions methods. Considering the solar cell power conversion efficiency and cost, low cost deposition such as CBD should be preferred. Table 2 gives the details of preparative parameters used to deposite CIS thin films using the CBD technique. In order to identify the desired phase compound, only XRD study is not sufficient.

4. Hydrothermal synthesis of CIS nanocrystals and their properties

Metal chalcogenide nanomaterials are the important class of materials, which are used in a variety of optoelectronic devices. Due to the quantum confinement effect and ability to tune the chemical composition, these nanomaterials show fascinating optoelectronic properties.[57] Among different metal chalcogenide materials, the copper indium disulfide (CIS) nanocrystals are interesting because of non-toxic, cadmium and lead-free, environmentally stable constituents. The CIS has a high absorption coefficient in the visible spectral range and a direct band gap of about 1.5 eV.[58] The CIS Bohr exciton radius is about 4 nm,[58] therefore the effect of quantum confinement in CIS nanocrystals can be observed. Thus, by changing the size of the CIS nanoparticles, the properties of absorption and emission can be tuned to the visible part of the spectrum.[59] Due to these fascinating properties, the CIS nanocrystals find applications in various fields including photocatalysis,[60] light emitting diodes (LEDs)[61] and particularly in different photovoltaic devices.[62,63] Numerous synthesis routes have been reported for the synthesis of CIS nanocrystals. Among them, colloidal synthesis,[64] hydrothermal synthesis, solvothermal synthesis,[65,66] and hot injection method[67,68] are the primary routes that require heat treatment during the synthesis. However, some room-temperature synthesis method is also developed and is attractive in minimizing the production cost and ensuring sustainability.[69,70]

4.1 Hydrothermal synthesis of CIS nanoparticles

Many nanocrystal synthesis approaches employ organic solvents, which are generally toxic in nature and may cause adverse environmental impact. Also, the synthesis technique requires high temperature and vacuum conditions. This undoubtably increases the cost. Because of this, the production is hardly scaled to industrial scale. Therefore, a facile and low-cost simple approach is highly desirable. Hydrothermal method is a low cost and simple method for the synthesis of variety of nanocrystals. In a hydrothermal method, the aqueous solution of precursors is heated in a sealed stainless-steel autoclave. High temperature (above boiling point of water) and high pressure (above atmospheric pressure) environment in sealed autoclave provide a single step process, which results in a high crystalline product. In this section, we present the hydrothermal method for the synthesis of CIS nanocrystal and their physical properties. Fig. 9 shows the schematics of the hydrothermal synthesis method of CIS nanoparticles.

Understanding the formation mechanism of the ternary $CuInS_2$ nanocrystals is incredibly complex due to different properties of Cu^+ and In^{3+} cations. In CIS, Cu^+ and S^{2-} ions are the soft Lewis and In^{3+} is a hard Lewis acid in the character, respectively.[71] Due to soft and hard Lewis acid characters of Cu and In, their reactivity to the sulfur is distinct. Therefore, it is necessary to balance the precursor's reactivity of both the cations to avoid the formation of binary phases. Furthermore, the CIS differs from the exact 1:1:2 ratio between copper, indium and sulfur. Therefore, stoichiometry is an additional parameter that is required to be adjusted by optimizing the synthesis parameters. Therefore, copper and indium's required reactivity can be achieved by employing different stabilizers in the reaction mixture.[67] There are very few reports on the synthesis of CIS nanocrystals using water-based, simple cost-effective hydrothermal methods. For example, Nayari *et al.*[72] synthesized $CuInS_2$ nanoparticles under different experimental conditions such as the use of various copper ($CuCl_2$, CuCl) and sulfur (CS_2 and S powder), different autoclave conditions (filling rate 80-90%) as well as different temperature conditions (150-250 °C). The sample obtained using CuCl, In metal and S powder at 220 °C and 80% of autoclave filling rate for 20 h of rection time showed the best

Table 2. Preparative parameters of the $CuInS_2$ thin film deposited using chemical bath deposition (CBD).

Sr. No	Precursors	Deposition Temperature	Substrate Material	Remark	Ref.
1	10 mL, $CuCl_2.H_2O$ (0.5 M) + 5.5 mL $InCl_3$ (0.5 M) + 40 mL $CS(NH_2)_2$, + 6 mL triethylamine (0.5 M) + 20 mL ammonia (13.4 M)	25, 45 and 80 °C	Glass	Investigation done on Effect of deposition time and deposition temperature on properties of the CIS thin films. The film deposited at lower temperature and at lower deposition time was non-uniform, while single phase CIS films were formed at 80 °C and 45 min of deposition time.	[19]
2	$CuSO_4.5H_2O$ + $In_2(SO_4)_3$ triethylamine (TEA) + hydrazine hydrate (HH) + Na_2S	RT	Glass	p-CIS films were deposited at room temperature using anionic precursor complexed with TEA and HH and Na_2S as a cationic precursor. Electrical resistivity was reported to be 10 Ωcm.	[47]
3	1.11 mL, $CuCl_2.H_20$ (0.4 M), + 1.11 mL, $InCl_3$ (0.4 M) + 0.56mL, +TAA (7.4 M). + TEA + $GaCl_3$ (0.4).	RT	Glass	Obtained Ga doped CIS thin films from the solution of containing $CuCl_2.H_20$ (0.4 M), $InCl_3$ (0.5M) and complexed with TEA and thioacetamide. Ga doping has resulted in the transition of n-type semiconductor to p-type semiconductor.	[48]
4	$CuCl_2.H_20$ (0.4 M), + $InCl_3$ (0.4 M) + TAA (0.4 M). + TEA + 0.4 M of $Zn(NO_3)_2$, $SbCl_3$, $Ni(NO_3)_2.6H_2O$.	RT	Glass	Zn, Sb, Ni-CIS thin films were deposited successfully using the CBD method at room temperature. The doped films were used to study hydrogen evolution. The report showed that Zn-CIS films showed a maximum hydrogen evolution.	[49]
5	$CuCl_2$, + $InCl_3$ + $CS(NH_2)_2$ + TEA, NH_3	65 °C	Glass	The optical bandgap of the chemically as-deposited film was 1.5eV. For the deposited film, Weak diffraction peak was recorded. The deposited films, heated at 700 K in sulfur atmosphere showed a bandgap value of 1.52eV. The electrical resistance of the as-deposited single-phase CIS indicates the extrinsic and intrinsic regions. Annealing in the sulfur vapor decreased resistivity.	[50]
7	$CuSO_4$(0.02M) + $InCl_3$ (0.02M) + ammonia + citric acid+ $(NH_2)_2CS$ (0.05M) + TEA (0.02M)	45 °C	Glass	The CIS nanorods of 200-250 nm with 20-38 nm diameters were synthesized using CBD method. The XRD showed intense peak at 37.32° orientated along the (211) crystal plane is the characteristics peak of CIS. SEM showed rod-like structure of the CIS. The conductivity of the sample was changed from n-type to p-type when etched in ammonia.	[53]
8	C_2H_5NS, (1.0 M) + $In(NO_3)_3$ (0.1 M)+ CH_3COOH (0.1 M)	RT	Glass	The CBD deposited In_2S_3-CuS films were completely transferred to CIS thin films after heat treatment at 350 °C for 24 hr. The device formed glass/SnO_2:F/CdS/Sb_2S_3/$CuInS_2$/PbS/C/Ag with CBD deposited CIS film showed 0.53% of photoconversion efficiency.	[54]
9	31.25 mL, $CuSO_4$ (0.1 M) + 25 ml, $InCl_3$ (0.1 M) + $Na_3C_6H_5O_7$ (0.1 M)	45 °C	ITO	As deposited films were amorphous. The film annealed at 450 °C showed crystalline chalcopyrite structure. Characteristics Raman peak was found at 290 cm^{-1} belong to chalcopyrite CIS.	[56]

[RT- Room temperature, TEA- Triethanolamine, TAA- Thioacetamide, ITO- Indium tin oxide] results. Xiao *et al*.[73] synthesized CIS nanorods using $CuCl_2$, In, CS_2, and NaOH as a reaction reagent. Role of attacking NaOH reagent is to release S^{2-} ions from sulfur source in the reaction process. Under the optimized condition of reaction temperature (180 °C) and reaction time (15 h), the CIS product exhibits nanorods 20-25 nm in diameter and 400-450 nm inlength. Hydrothermally synthesized CIS nanoparticle were used for photocatalytic nitrate reduction in aqueous solution.[74] The aggregated nanosized CIS nanocrystals (Fig. 10(a)) of large BET surface of 9.8 m^2/g showed significant photocatalytic nitrate reduction (74.8%) after 2h of irradiation. Fig. 10(b) shows the comparison of photocatalytic activity of hydrothermal synthesized CIS nanoparticles (HY) with the that of the high temperature solid state reaction (SSR) synthesized CIS nanoparticles.

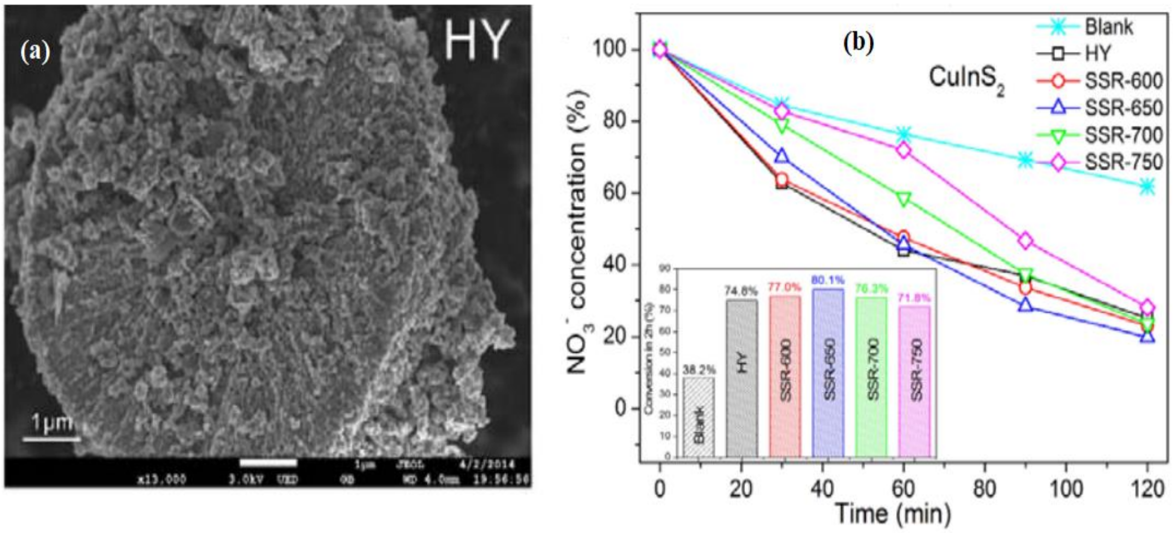

Fig. 10 a) SEM image of hydrothermal synthesized CIS sample, b) The time dependence of the photocatalytic nitrate reduction for hydrothermal synthesized $CuInS_2$ samples, reproduced with the permission from [74].

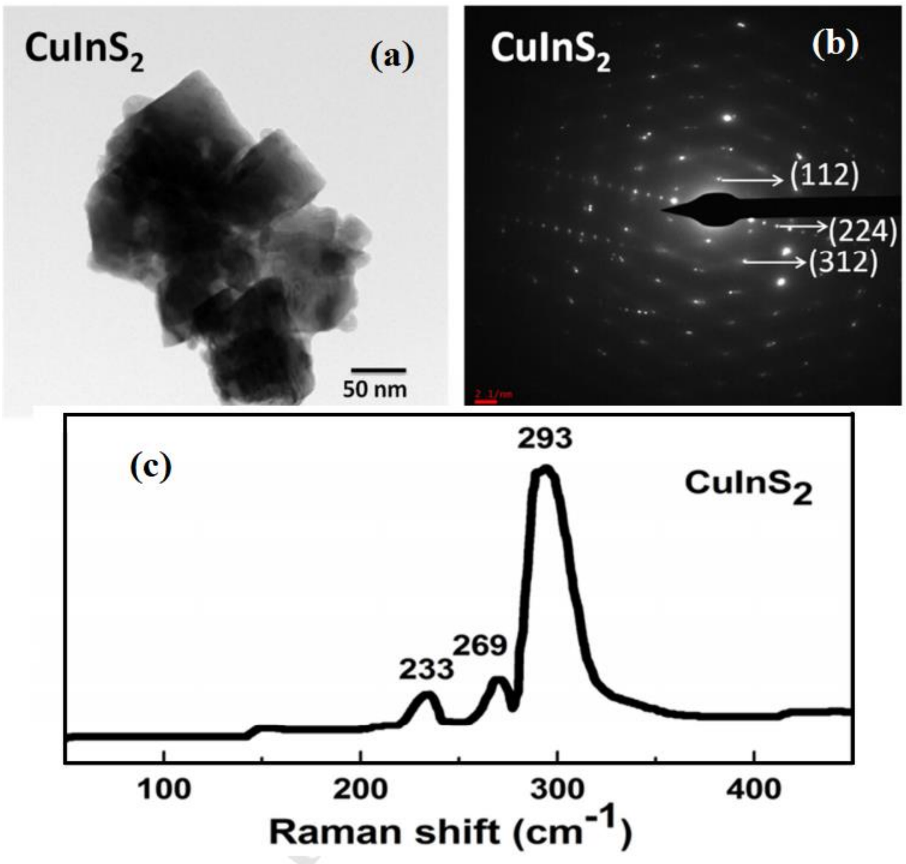

Fig. 11 a) TEM b) SAED patterns of as $CuInS_2$ nanotubes, c) Raman spectra of as $CuInS_2$ nanotube , reproduced with the permission from [75].

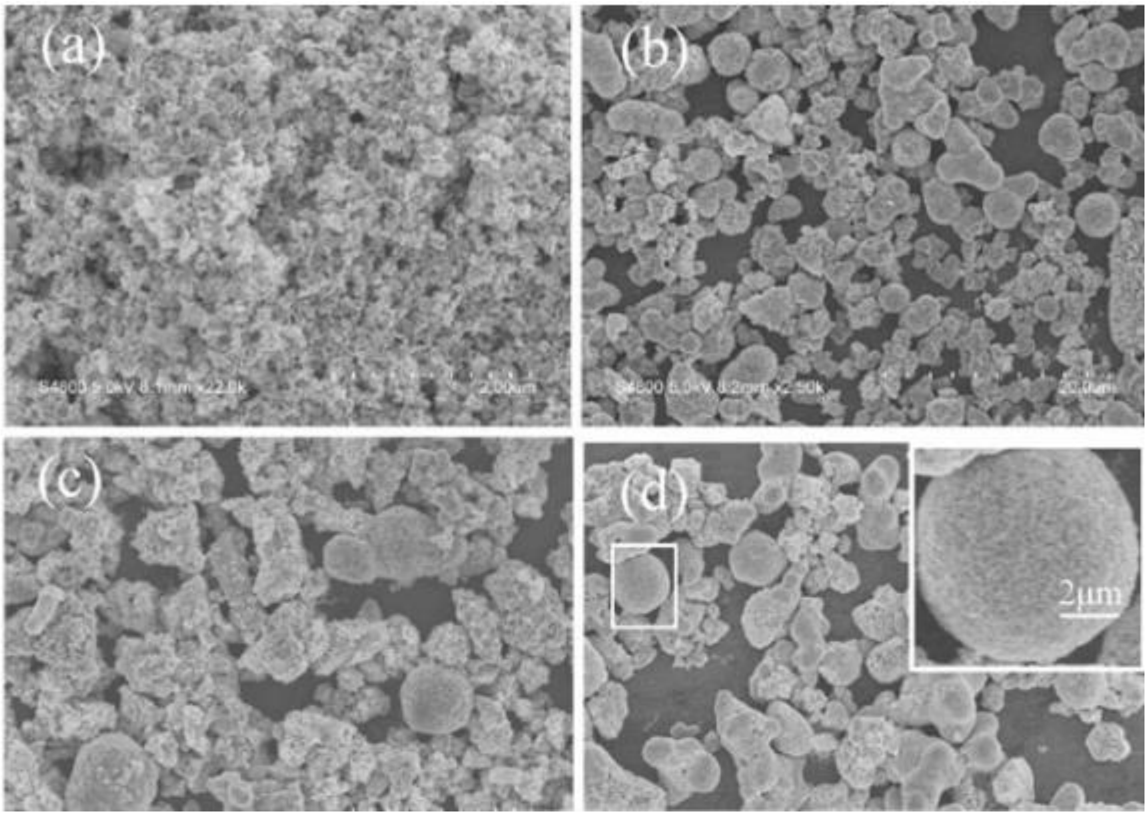

Fig. 12. FESEM images of the as-synthesized $CuInS_2$ samples incubated at 160 °C for a) 4, b) 8, c) 12, and d) 24 h, reproduced with permission from [78].

Sugan *et al.*[75] reported the hydrothermal synthesis of tetragonal chalcopyrite CIS nano-cubes with structure highly oriented along characteristics (112) peak (Fig. 11(a,b)). The Raman spectrum of the CIS sample is shown in Fig. 11(c). The CIS exhibits three vibrational Raman peaks located around 293, 269 and 233 cm^{-1}. The dominant peak at 293 cm^{-1} can be assigned to A1 mode and other peaks at 269 and 233 cm^{-1} may be attributed to E(LO/TO) and B_2(LO/TO) modes.[76,77]

Chang *et al.*[78] synthesized porous like microspheres of CIS structure using Gemini as a surfactant in the starting solution. Gemini surfactant possess essential characteristics that it can be used as a soft molecular template to control the structural and morphological properties of many inorganic nanomaterials.[79,80] The effect of Gemini template on morphology of CIS nanoparticles is shown in field emission scanning electron microscopy (FESEM), Fig. 12. This indicates that the aggregated nanoparticles get changed to porous-microspheres as the reaction time is increased.

5. Conclusion and future scope

The present review outlines the preparative parameters and the physical properties of the CIS absorber layer deposited via CBD method. The CIS deposition has been reported at different temperatures of the precursor solution. However, reports on room temperature deposition of CIS thin-film are limited. The room temperature deposition leads to amorphous, non-stoichiometric film composition. For low-temperature deposition, proper optimization of preparative parameters and understanding of suitable solution chemistry are required. The crystalline nature of the CIS film can be enhanced by annealing the film at different temperatures. Annealing in sulfur vapor atmosphere enhances the conductivity of CIS film. It is reported that the conductivity of the CBD deposited sample changed from n-type to p-type after doping with Ga, Sb or Ni. Etching the CIS film in ammonia also changed the conductivity. As an absorber material in solar cell application, the required grain size of CIS film must have a value of around 1-2 µm. However, it is found difficult to obtain the required grain size of CIS material using CBD. The deposition parameters should be properly optimized to get the desired thickness of the film. Considering the photo conversion efficiency and cost of the solar cell, low-cost deposition such as CBD should be preferred. Another important aspect in CBD method is the pH of the cationic and anionic precursor solution. The CIS can be deposited both in acidic as well as in basic medium. A simple and cheaper deposition technique, such as CBD, onto cheaper and flexible substrates could effectively revive the advancements of cells. Chemical synthesis method is low-cost and simple for the synthesis of CIS nanocrystals. The electrical and optical properties shown by chemically synthesized CIS nanoparticles are interesting for solar energy conversion.

Supporting information

Not applicable

Conflict of interest

There are no conflicts to declare.

References

[1] IEEJ Outlook 2020, The Institute of Energy Economics, Japan IEEJ © 2010

[2] G. Balachandar, N. Khanna, D. Debabrata, Biohydrogen, (Second Edition), Biomass, Biofuels, Biochemicals, 2019 (2019) 79-122.

[3] W. Soetaert and E. J. Vandamme, Biofuels, John Wiley and Sons Ltd., Great Britan, 2009, 1e8, doi: 10.1002/star.200990030.

[4] UNEP, Global Environment Outlook, 2004/05, https://na.unep.net/atlas/datlas/sites/default/files/GEO-4_Report_Full_en.pdf.

[5] E. Radziemska, *Prog. Energy Combust. Sci.*, 2003, **29**, 407, doi: 10.1016/S0360-1285(03)00032-7.

[6] L. Li, T. Zhai, Y. Bando and D. Golberg, *Nano Energy*, 2012,**1,** 91, doi: 10.1016/j.nanoen.2011.10.005.

[7] J. Cen, Q. Wu, D. Yan, J. Tao, K. Kisslinger, M. Liu and A. Orlov, *Phys. Chem. Chem. Phys.*, 2017, **19**, 2760, doi: 10.1039/C6CP07111B.

[8] D. C. Look and J. C. Manthuruthil, *J. Phys. Chem. Solids*, 1976, **37,** 173, doi: 10.1016/0022-3697(76)90157-8.

[9] K. Yoshino, T. Ikari, S. Shirakata, H. Miyake and K. Hiramatsu, *Appl. Phys. Lett.*, 2001, **78**, 742, doi: 10.1063/1.1345802.

[10] J. Lee and C. S. Han, *Nanoscale Res. Lett.*, 2014, **9**, 78, doi: 10.1186/1556-276X-9-78.

[11] Q. Guo, S. J. Kim, M. Kar, W. M. Shafarman, R. W. Birkmire, E. A. Stach, R. Agrawal and H. W. Hillhouse, *Nano Lett.*, 2008, **8**, 2982, doi:10.1021/nl802042g.

[12] L. Li, N. Coates and D. Moses, *J. Am. Chem. Soc.*, 2010, **132**, 22-23, doi: 10.1021/ja908371f

[13] X. Tang, W. Cheng, E. S. G. Choo and J. Xue, *Chem. Commun.*, 2011, **47,** 5217, doi: 10.1039/C1CC10417A.

[14] J. Lee and C. S. Han, *Nanoscale Res. Lett.*, 2014, **9**, 78, doi: https://doi.org/10.1186/1556-276X-9-78.

[15] H. Bihri and M. Abd-Lefdil, *Thin Solid Films*,1999, **354**, 5, doi: 10.1016/S0040-6090(99)00433-2

[16] J. M. Meese, J. C. Manthuruthil and D. R. Locker, *Bull. Am. Phys. Soc.*, 1975, **20,** 696.

[17] D. Braunger, D. Hariskos, T. Walter and H. Schock, *Sol. Energy Mater. Sol. Cells*, 1996, **40**, 97, doi: 10.1016/0927-0248(95)00069-0.

[18] J. Klaer, J. Bruns, R. Henninger, K. Siemer, R. Klenk, K. Ellmer and D. Braunig, *Semicond. Sci. Technol.*, 1998, **13**, 1456, doi: 10.1088/0268-1242/13/12/022.

[19] G. K. Padam and S.U.M. Rao, *Sol. Ener. Mater.*, 1986, **13**, 297, doi: 10.1016/0165-1633(86)90004-3.

[20] S. Lugo, I. Lopeza, Y. Penaa, M. Calixtob, T. Hernandeza, S. Messinac and D. Avellanedad, *Thin Solid Films*, 2014, **569,** 76, doi: 10.1016/j.tsf.2014.08.040.

[21] F. De Moure-Flores, A. Guillen-Cervantes, E. Campos-Gonzalez, J. Santoyo-Salazar, J. S. Arias-Ceron, J. Santos-Cruz, S. A. Mayen-Hernandez, M. L Olvera., J. G. Mendoza-Alvarez, O. Zelaya-Angel and G. Contreras-Puente, *Mater. Sci. Semicond. Process.*, 2015, **39**, 755, doi: 10.1016/j.mssp.2015.06.053.

[22] E. Aydin and N. D. Sankir, *Int. J. Electrochem. Sci.*, 2017, **12,** 969, 10.20964/2017.10.80.

[23] P. Dube, A. O. Uma and C. M. Muiva, *Ceram. Int.*, 2020,**46**,7396, doi: 10.1016/j.ceramint.2019.11.235.

[24] A. Chihi and B. Bessais, *RSC Advances*, 2017, **7**, 29469, doi: 10.1039/C7RA04330A.

[25] B. Maheswari and M. Dhanam, *Mater. Sci.-Poland*, 2013, **31**, 193, doi: 10.2478/s13536-012-0094-0.

[26] H. M. Pathan, C. D. Lokhande, *Bull. Mater. Sci.*, 2004, **27**, 85, doi: 10.1007/BF02708491.

[27] B. R. Sankapal, A. Ennaoui, T. Guminskaya, T. Dittrich, W. Bohne, J. Rohrich, M. C. Lux-Steiner, *Thin Solid Films*, 2005, **142**, 480-481, doi: 10.1016/j.tsf.2004.11.020.

[28] K. Siemer, J. Klaer, I. Luck, J. Bruns, R. Klenk, D. Braunig, *Sol. Energy Mater. Sol.*, 2001, **67, 159-**166, doi: 10.1016/S0927-0248(00)00276-2.

[29] M. Gossla, H. Metzner, H.-E. Mahnke, *Thin Solid Films*, 2001, **387,** 77, doi: 10.1016/S0040-6090(01)00788-X.

[30] H. Metzner, Th. Hahn, J.-H. Bremer, M. Seibt, B. Plikat, I. Dirnstorfer, B.K. Meyer, *Thin Solid Films*, 2000, **504**, 361, doi: 10.1016/S0040-6090(99)00804-4.

[31] W. Calvet, , C. Lehmann, T. Plake, C. Pettenkofer, *Thin Solid Films*, 2005, **347**,480-481, doi:10.1016/j.tsf.2004.11.090

[32] J. Eberhardt, H. Metzner, R. Goldhahn, F. Hudert, U. Reislöhner, C. Hülsen W. Witthuhn, *Thin Solid Films*, 2005, **415,** 480-481, doi: 10.1016/j.tsf.2004.11.089.

[33] M. Gossla, T. Hahn, H. Metzner, J. Conrad, U. Geyer, *Thin Solid Films*, 1995, 268, 39, 10.1016/0040-6090(95)06870-8.

[34] J. D. Harris, K. K. Banger, D. A. Scheiman, M. A. Smith, M.H.-C. Jin, A.F. Hepp, *Mater. Sci. Eng. B*, 2003, **98**, 150, doi: 10.1016/S0921-5107(03)00041-2.

[35] W. J. Tsaia, C. H. Tsaia, C. H. Changa, J. M. Tinga, R. R. Wang *Thin Solid Films*, 2010, **519**, 1712, doi:10.1016/j.tsf.2010.08.086.

[36] I. E. Kacher, A. K. Shuaibov, M. Y. Rigan, A. I. Dashchenko, *High Temp.*, 2002, **40**, 814, doi: 10.1023/A:1021412930269.

[37] M. Nanu, L. Reijnen, B. Meester, A. Goossens, J. Schoonman, *Thin Solid Films*, 2003, **492,** 431-432, doi: 10.1016/S0040-6090(03)00230-X.

[38] J. E. Jaffe, A. Zunger, *Phys. Rev. B*, 1984, **29,** 1882, doi: 10.1103/PhysRevB.29.1882.

[39] J. E. Jaffe, A. Zunger, *Phys. Rev. B*, 1983, **28,** 5822, doi: 10.1103/PhysRevB.28.5822.

[40] J. J. M Binsma. L. J. Giling J. Bloem J. Crys.t Growth, 1980, **50**, 429, doi: 10.1016/0022-0248(80)90090-1.

[41] F. J. Blatt, Physics of Electronic conduction in solids, Mc. Graw-Hill, New York, 1968, 19.

[42] H. Z. Zhong, Z. L. Bai, B. S. Zou, *J. Phy. Chem. Lett.*, 2012, **3**, 3167, doi: 10.1021/jz301345x.

[43] H. Hahn, G. Frank, W. Klinger, A. D. Meyer, G. Storger, *Anorg. allg. Z. Chemie*, 1953, **271**, 153, 10.1002/zaac.19532710307.

[44] R. S. Mane, C.D. Lokhande, *Mater. Chem. Phys.*, 2000, **65,**

1, doi: 10.1016/S0254-0584(00)00217-0.
[45] G. Hodes, Chemical Solution deposition of semiconductor films, Marcel Dekker, Inc., 2003 Page -31.
[46] H. M. Pathan, C. D. Lokhande, *Appl. Surf. Sci.*, 2004, **239**, 11, doi: 10.1016/j.apsusc.2004.04.003.
[47] S. J. Roh, S. M. Mane, H. M. Pathan, O. S. Joo, S. H. Han, *Appl. Surf. Sci.*, 2005, 252, 1981, doi: 10.1016/j.apsusc.2005.02.140.
[48] G. T. Pan, M. H. Lai, R. C. Juang, T. G. Chung, T. C.Yang, *Sol. Energy Mater. Sol.*, 2010, **94**, 1790, doi: 10.1016/j.solmat.2010.05.047.
[49] E. Garskaite, G. T. Pan, T. C. Yang, S. T. Haung, A. Kareiva, *Solar energy*, 2012, **86,** 2584, doi: 10.1016/j.solener.2012.05.031.
[50] S. Mahmoud, A. Hamid Eid, *Fizaka A*, 1997, **6,** 171.
[51] H. Neumann, W. Horig, V. Savelev, J. Lagzdonis, B. Schumann, G. Kuhn, *Thin Solid Films*, 1981, **79**, 167, doi: 10.1016/0040-6090(81)90275-3.
[52] S. Bini, K. Bindu, M. Lakshmi, C. S. Kartha, K. P. Vijayakumar, Y. Kashiwaba, T. Abe, *Renew. Energy*, 2000, **20**, 405, doi:10.1016/S0960-1481(99)00122-6.
[53] S. Ramphal, S. Suyeon, R. S. Mane, T. Ganesh, A. Ghule, C. Gangri, D. Ham, S. Min, L. Wonjoo, S. Han, *Mater. Chem. Phys.*, 2009, 116, 28, doi: 10.1016/j.matchemphys.2009.02.003.
[54] S. Lugo, I. Lopez, Y. Pena, M. Calixto, T. Hernandez, S. Messina, D. Avellaneda, *Thin Solid Films*, 2014, **569**, 76, doi: 10.1016/j.tsf.2014.08.040.
[55] D. C. Nguyen, K. Takehara, T. Ryo, S. Ito, *Energy Procedia*, 2011, **10**, 49, doi: 10.1016/j.egypro.2011.10.151.
[56] F. Cui, L. Wang, X. Chen, X. Sheng, D. Yang, Y. Sun, *Proceedings of SPIE - the International*, 2008, doi: 10.1117/12.792396
[57] S. R. Thomas, C. W. Chen, M. Date, Y. C. Wang, H. W. Tsai, Z. M. Wang, Y.L. Chueh, *RSC Adv.*, 2016, **6**, 60643, doi:10.1039/C6RA05502H.
[58] D. Aldakov, A. Lefrançois, P. Reiss, *J. Mater. Chem. C*, 2013, **1**, 3756, doi: 10.1039/C3TC30273C.
[59] S. V. Kershaw, A. S. Susha, A. L. Rogach, *Chem. Soc. Rev.*, 2013, **42**, 3033, doi: 10.1039/C2CS35331H.
[60] J. Jiea, W. Zhang, I. Bello, C.-S. Lee, S.-T. Lee, *Nano Today*, 2010, **5,** 313, doi: 10.1016/j.nantod.2010.06.009.
[61] R. Xie, M. Rutherford, X. Peng, *J. Am. Chem. Soc.*, 2009, **131**, 5691, doi: 10.1021/ja9005767.
[62] B. Tell, J. L. Shay, H. M. Kasper, *Phys. Rev. B*, 1971, **4,** 2463, doi: 10.1103/PhysRevB.4.2463.
[63] S. Khanchandani, S. Kumar, A. K. Ganguli, *ACS Sustainable Chem. Eng.*, 2016, **4**, 1497, doi: 10.1021/acssuschemeng.5b01460.
[64] J. E. Halpert, F. S. F. Morgenstern, B. Ehrler, Y. Vaynzof, D. Credgington, N. C. Greenham, *ACS Nano*, 2015, **9**, 5857, doi: 10.1021/acsnano.5b00432.
[65] M. Arar, M. Gruber, M. Edler, W. Haas, F. Hofer, N. Bansal, L. X. Reynolds, S. A. Haque, K. Zojer, G. Trimmel, T. Rath, *Nanotech.*, 2013, **24**, 484005, doi: 10.1088/0957-4484/24/48/484005.
[66] C. Krause, D. Scheunemann, J. Parisi and H. Borchert, *J. Appl. Phys.*, 2015, **118**, 205501, doi: 10.1063/1.4936198.
[67] W. C. Huang, C. H. Tseng, S. H. Chang, H. Y. Tuan, C. C. Chiang, L. M. Lyu and M. H. Huang, *Langmuir*, 2012, **28,** 8496, doi: 10.1021/la300742p.
[68] H. Lewerenz., *J. Sol. Energy Mater. Sol. Cells*, 2004, **83,** 395, doi: 10.1016/j.solmat.2004.02.034.
[69] Y. Jiang, Y. Wu, X. Mo, W. Yu, Y. Xie and Y. Qian, *Inorg. Chem.*, 2000, **39**, 2964, doi: 10.1021/ic000126x.
[70] R. Xie, M. Rutherford and X. Peng, *J. Am. Chem. Soc.*, 2009, **131,** 5691, doi: 10.1021/ja9005767.
[71] X. Sheng, L. Wang and D. Yang, *J. Sol−Gel Sci. Technol.*, 2012, **62**, 87, doi: 10.1007/s10971-012-2689-7.
[72] T. Nyaria, P. Barvinschi, R. Baies, P. Vlazan, F. Barvinschi and I. Dekany, *J. Cryst. Growth*, 2005, **275**, e2383, doi: 10.1016/j.jcrysgro.2004.11.343
[73] J. Xiao, Y. Xie, R. Tang and Y. Qian, *J. Solid State Chem.*, 2001, **161**, 179, doi: 10.1006/jssc.2001.9247.
[74] Y. Wang, J. Yang, W. Gao, R. Cong and T. Yang, *Mater.Lett.*, 2014, **137**, 99, doi: 10.1016/j.matlet.2014.08.144.
[75] S. Sugan, K. Baskar and R. Dhanasekaran, *Curr. Appl. Phys.*, 2014, **14**,1416, doi: 10.1016/j.cap.2014.08.011.
[76] W. H. Koschel, M. Bettini, *Phys. Stat. Sol B.*, 1975, 72, 729, doi: 10.1002/pssb.2220720233.
[77] H. Matsushita, S. Endo, T. Irie, *Jpn. J. Appl. Phys.*, 1992, **31,** 18, doi: 10.1143/JJAP.31.18.
[78] W. G. Chang and L. L. Tao, *J. Appl. Spectrosc.*, 2019, **86,** 549, doi: 10.1007/s10812-019-00857-7.
[79] M. S. Bakshi, F. Possmayer and N. O. Petersen, *Chem. Mater.*, 2007, **19**, 1257, doi: 10.1021/cm062771t.
[80] M. S. Bakshi, F. Possmayer, N. O. Petersen, *J. Phys. Chem. C*, 2008, **112,** 8259, doi: 10.1021/jp801306x.

Author information

Mr. Jitendra P. Sawant

Mr. Jitendra P. Sawant is an assistant professor at University Department of Physics, Mumbai University, Mumbai, India. He received his master degree in solid state physics, from Shivaji University, Kolhapur, Maharashtra India. He submitted his Ph.D. thesis to Mumbai university. His research interest includes, thin films, solar cells, catalysis, nanomaterial

Dr. Shoyebmohamad F. Shaikh

Dr. Shoyebmohamad F. Shaikh is an Assistant professor in King Saud University, Riyadh, Saudi Arabia. He completed is Ph.D. degree in Clean Energy and Chemical Engineering from UST (University of Science and Technology), South Korea for which I worked in Korea Institute of Science and Technology, Seoul, South Korea during 2010-2015. During Ph. D. course his major concern was to enhance the power conversion efficiency of metal oxide-based nanostructures in Dye Sensitized Solar cells. For that various surface modifications were attempted by considering band gap engineering kinetics. He has one-year Postdoctoral experience in perovskite solar cell, Yonsei University, South Korea during academic year 2015-2016. His research interest on electrochemical supercapacitors, gas sensor and water spitting by using conducting polymers, metal oxide and carbon-based materials.

Dr. Rohidas B. Kale

Dr. Rohidas B. Kale is currently working as an Associate Professor at The Institute of science, Fort, Mumbai Maharashtra. He obtained his Ph.D.in 2005 from Shivaji University, Kolhapur, Maharashtra, India. He was a visiting scientist at National Tsing-Hua University, Taiwan (2006-2007). He established a Thin Film Physics lab at Institute of Science. He has around 50 publication and about 1381 citations. His research interest is on nanomaterials, semiconductor, luminescent materials.

Dr. Habib M. Pathan

Dr. Habib M. Pathan is an assistant professor at the Department of Physics, Savtribai Phule Pune University Pune. He obtained his Ph.D. in 2003 from Shivaji University, Kohlapur. He was a visiting scientist (2004-2007) at Korea Institute of Science and Technology (KIST), South Korea. He has joined Department of Physics, Savtribai Phule Pune University Pune in 2008, and established a new research laboratory namely "Advanced Physics Laboratory" and actively engaged in teaching and research. His research focused on thin-film deposition, nanostructured material for Dye sensitised solar cells and supercapacitor applications, PEC hydrogen Generation. He has about 205 scientific publications, 04 patents, and 2640 citations. He is a Life Member of Material Research Society of India. He was a visiting professor at Chonbuk National University Iksan, South Korea.